



Climatology and atmospheric conditions associated with cool season bow echo storms in Poland

Daniel Celiński-Mysław^{a,*}, Angelika Palarz^a, Mateusz Taszarek^b

^a Department of Climatology, Jagiellonian University, Gronostajowa 7, 30-387 Krakow, Poland

^b Department of Climatology, Adam Mickiewicz University, Bogumiła Krygowskiego 10, 61-680 Poznań, Poland

ARTICLE INFO

Keywords:

Bow echo
Severe wind gusts
Cool season
Thunderstorm
Poland

ABSTRACT

Cool season severe wind events may be related to the occurrence of mesoscale convective systems with a bow echo (i.e. arch-shaped band of radar reflectivity). This research provides an insight into the spatial and temporal distribution of bow echoes occurring in the cool season (October–March) between January 2007 and March 2019 over Poland and presents atmospheric conditions (synoptic, kinematic, and thermodynamic) associated with such events. The analysis has been performed utilizing SYNOP (surface observations), ESWD (European Severe Weather Database), radar (CMAX, CAPP), reanalysis (ERA-5) and sounding data. During the period studied, 27 Cool Season Bow Echoes (CSBEs) were identified across Poland. The area most exposed to the occurrence of CSBEs included south-western Poland, while the north-eastern and eastern part of the country was generally free of this phenomenon. Unlike the warm season cases, CSBEs do not indicate a clear diurnal cycle. As our results have shown, a high shear/low CAPE (Convective Available Potential Energy) environment in combination with a triggering mechanism along the cold front (frontal cases) or along the surface trough (post-frontal cases) can be considered as supportive for CSBE. Such cases were always associated with the presence of strong air flow in the low and mid troposphere. The analysis of 500 hPa geopotential height fields revealed that troughs (often with embedded smaller-amplitude dynamic waves) moving over Central Europe were present in 26 out of 27 cases. The median value of vertical wind shear for identified cases exceeded 30 m/s for deep-layer shear (DLS), was well above 20 m/s for mid-level shear (MLS), and higher than 17 m/s for low-level shear (LLS). A recurring finding was also that post-frontal cases formed in an environment with weaker shear, but higher CAPE.

1. Introduction

Cool season convective lines may be responsible for the occurrence of widespread damaging winds and tornadoes (e.g. Gatzen, 2011; Sherburn et al., 2016; Earl et al., 2017; Gatzen et al., 2019). These phenomena are frequently related to the occurrence of convective systems with a bow echo (i.e. arch-shaped band of high radar reflectivity; Burke and Schultz, 2004; Trapp et al., 2005; Celiński-Mysław and Matuszko, 2014). Current research on the spatial and temporal variability of Cool Season Bow Echoes (CSBEs) and derechoes concerns primarily the area of the USA (e.g. Burke and Schultz, 2004; Klimowski et al., 2004; Adams-Selin and Johnson, 2010) and only few such studies have been performed for other parts of the world (e.g. Kounkou et al., 2009; Clark, 2013; King et al., 2017). So far, European studies on CSBE and derecho have focused mainly on the environmental patterns related to case studies (Gatzen et al., 2011; Celiński-Mysław and Matuszko,

2014; Ludwig et al., 2015; Mathias et al., 2019).

The atmospheric conditions associated with bow echo and derecho events in Europe were determined using synoptic and sounding observations (e.g. Gatzen et al., 2011; Púčik et al., 2011; Celiński-Mysław and Matuszko, 2014; Celiński-Mysław and Palarz, 2017), models and reanalysis datasets (e.g. Punkka et al., 2006; Gospodinov et al., 2015; Celiński-Mysław et al., 2018) or hindcast experiments (Toll et al., 2015; Mathias et al., 2019; Taszarek et al., 2019). Previous research showed evidence that most warm season bow echo cases (April - September) over Central and Western Europe were associated with convective systems which had developed along the convergence zone (in a warm sector of a low) or in an articulated atmospheric front with a secondary active depression (e.g. Celiński-Mysław and Palarz, 2017; Mathias et al., 2017; Taszarek et al., 2019). The cold front of deep low pressure system with unstable air mass supported by a strong synoptic-scale lift (Gatzen et al., 2011; Celiński-Mysław and Matuszko, 2014; Ludwig

* Corresponding author.

E-mail addresses: daniel.celinski-myslaw@doctoral.uj.edu.pl (D. Celiński-Mysław), angelika.palarz@doctoral.uj.edu.pl (A. Palarz), mateusz.taszarek@amu.edu.pl (M. Taszarek).

<https://doi.org/10.1016/j.atmosres.2020.104944>

Received 12 September 2019; Received in revised form 15 January 2020; Accepted 6 March 2020

Available online 07 March 2020

0169-8095/ © 2020 The Authors. Published by Elsevier B.V. This is an open access article under the CC BY-NC-ND license (<http://creativecommons.org/licenses/by-nc-nd/4.0/>).

et al., 2015) or surface pressure trough in a postfrontal air masses (Mathias et al., 2019), in turn, may be conducive to the development of bow echoes and derechos in the cool season.

Previous works, dealing with the climatology and atmospheric conditions of cool season severe convective wind events in Europe, show evidence that kinematic and thermodynamic conditions are usually different in comparison to warm season cases. In the cool season, the environment is predominantly characterized by weak instability (small or negligible Convective Available Potential Energy – CAPE) and strong vertical wind shear (e.g. Clark, 2009, 2013; Gatzen, 2011; Celiński-Mysław and Matuszko, 2014; Púčik et al., 2015; Mathias et al., 2019). However, as the squall-line simulations provided by Jewett and Wilhelmson (2006) revealed, the pre-storm environments characterized by low CAPE and high shear do not usually produce severe, long-lasting convection when the large-scale environmental forcing is lacking.

Warm season convective wind events can form both in weakly and strongly forced environments. However, shear-related parameters during spring and summer are usually much lower compared to the cool half of the year (e.g. Taszarek et al., 2018). Previous results also confirmed markedly higher CAPE values for convective windstorms occurring over the United States, compared to Central Europe (e.g. Evans and Doswell III, 2001; Klimowski et al., 2004; Burke and Schultz, 2004; Kuchera and Parker, 2006; Cohen et al., 2007; Púčik et al., 2015; Taszarek et al., 2017; Celiński-Mysław et al., 2018). However, as evidenced in the above-listed studies, in both Europe and the United States, severe long-lived bow echoes can form even when CAPE is very low.

Considering the mode of bow echo development, the previous research revealed that, irrespective of the area of occurrence, convective systems with a bow echo develop primarily as a result of squall line transformation or the evolution of often weakly organized convective cells (Burke and Schultz, 2004; Celiński-Mysław and Palarz, 2017). The predominant bow echo types, in turn, included classic bow echo and bow-echo complex (Klimowski et al., 2004, 2004; Celiński-Mysław and Palarz, 2017).

This study presents a climatology of CSBEs in Poland as prior elaborations did not focus on the topic within this part of Europe. The main aim is to determine the spatiotemporal distribution of CSBEs, as well as, to identify synoptic, kinematic, and thermodynamic conditions associated with such events. Through investigation of bow echo frequency and the knowledge about accompanying atmospheric conditions may possibly leading to advances in their forecasting in Poland. The article is structured as follows: the data and methods utilized for the study are described in Section 2. The climatology and environmental patterns associated with CSBEs are provided in section 3. Discussion and Conclusions are presented in Sections 4 and 5, respectively.

2. Data and methods

2.1. The identification of bow echo

The research focuses on the occurrence of bow echo in the cool season (i.e. early October till late March). The time series spanned a period from early January 2007 to late March 2019. Convective storms were classified as a bow echo following the same identification criteria as applied in Celiński-Mysław and Palarz (2017). These criteria include six essential points: (1) severe wind gusts accompanying the convective system movement (Fujita, 1978) (≥ 24 m/s or tornado), (2) bow or crescent-shaped radar echo (Fujita, 1978) (Fig. 1), (3) a tight reflectivity gradient at the leading edge (Klimowski et al. 2000, 2004), (4) an area with reduced reflectivity (Rear Inflow Notch – RIN) in the rear of a convective system (Fujita, 1978), (5) an increasing radius with time or a persistent arc (Klimowski et al. 2004; Burke and Schultz, 2004), and (6) time of existence of at least 30 min (Klimowski et al. 2004;

Gatzen 2013). The last criterion aims to exclude short-lived conglomerations of storms which do not constitute organized convective lines with a bow echo.

Burke and Schultz (2004) showed that no reports of severe wind gusts were recorded in only 6 of 150 hypothetical CSBEs. Therefore, similar to Celiński-Mysław and Palarz (2017), the first step in the methodology was to identify the periods in which severe wind gusts and tornadoes were recorded (then for these dates radar data was investigated to identify bow echo). The wind reports used in this study included data from the synoptic weather station network operated by the Polish Institute of Meteorology and Water Management (we also used data from stations located abroad in the immediate vicinity of the Polish border) and from the European Severe Weather Database (<http://www.eswd.eu/>). The vast majority of the 602 cases of severe wind events that occurred in the cool season in Poland was likely not associated with convection. Non-convective severe wind gusts were usually linked to large horizontal pressure gradient accompanying travelling cyclones over Central Europe, as well as the foehn effects within mountains over southern Poland. Non-convective cases were identified by comparing severe wind reports with radar (POLRAD – Polish radar network), satellite (IR 10.8, color-enhanced IR 10.8), and lightning data (PERUN lightning detection network).

The assessment of the remaining (from 2nd to 6th) criteria fulfillment was made by analyzing radar data for selected cases of severe wind events (for further details on this methodology, see Celiński-Mysław and Palarz (2017)). These data included collective radar maps for the area of Poland on the basis of CMAX (Column Maximum echo reflectivity) and CAPPI (Constant Altitude Plan Position Indicator) products (Centre for Ground Based Remote Sensing - Institute of Meteorology and Water Management). The POLRAD radar network consists of eight C-band Doppler radars: Meteor 500C (Poznań, Brzuchania, Świdwin), Meteor 1500C (Legionowo, Gdańsk), and dual-polarimetric Meteor 1600C (Pastewnik, Rzeszów, Ramża) of Selex ES. Further details on the network are available in Ośródkę et al. (2014).

Similarly as in Gatzen et al. (2011), Clark (2013) or Celiński-Mysław and Palarz (2017), the identification of radar-derived organizational patterns was accomplished through subjective analysis (manually labeled features/signatures extracted from radar images). A convective line was classified as a bow echo only if one or more wind reports could be unambiguously attributed to the line (wind reports coincided in time with the passage of convective systems rather than with a maximum pressure gradient or foehn effect) and after meeting remaining criteria. The beginning of bow echo was defined as the time of the first appearance of a 35-dBZ within a bow-shaped structure. The time of its strong dispersion or significant reduction of radar reflectivity, in turn, was considered as the bow echo's end.

2.2. Classifying types

Once a bow echo was confirmed, its type was determined. The type of bow echo was assigned based on morphological features identified on the radar image and in accordance with the classification proposed in Celiński-Mysław and Palarz (2017). Thus, each case was classified as one of five types: classic bow echo – BE (cases of a size larger than single storm cells, which are not linked to other organized convection), bow-echo complex – BEC (the bow echo is the primary, but not the only, organized convective structure – supercells or other linear complexes could additionally occur), cell bow echo – CBE (cases of the smallest sizes (10–25 km)), squall line bow echo – SLBE (elongated mesoscale convective systems with a bow echo with the length to width ratio of at least 5:1), and double bow echo – DBE (massive bows inside two mesoscale convective systems connected to each other for a period of time).

Taking into account the synoptic situation, we classified bow echo cases as frontal or post-frontal (as in Clark, 2013) by comparing surface analysis chart archives (available at 6-hourly intervals – [2](http://www.</p>
</div>
<div data-bbox=)

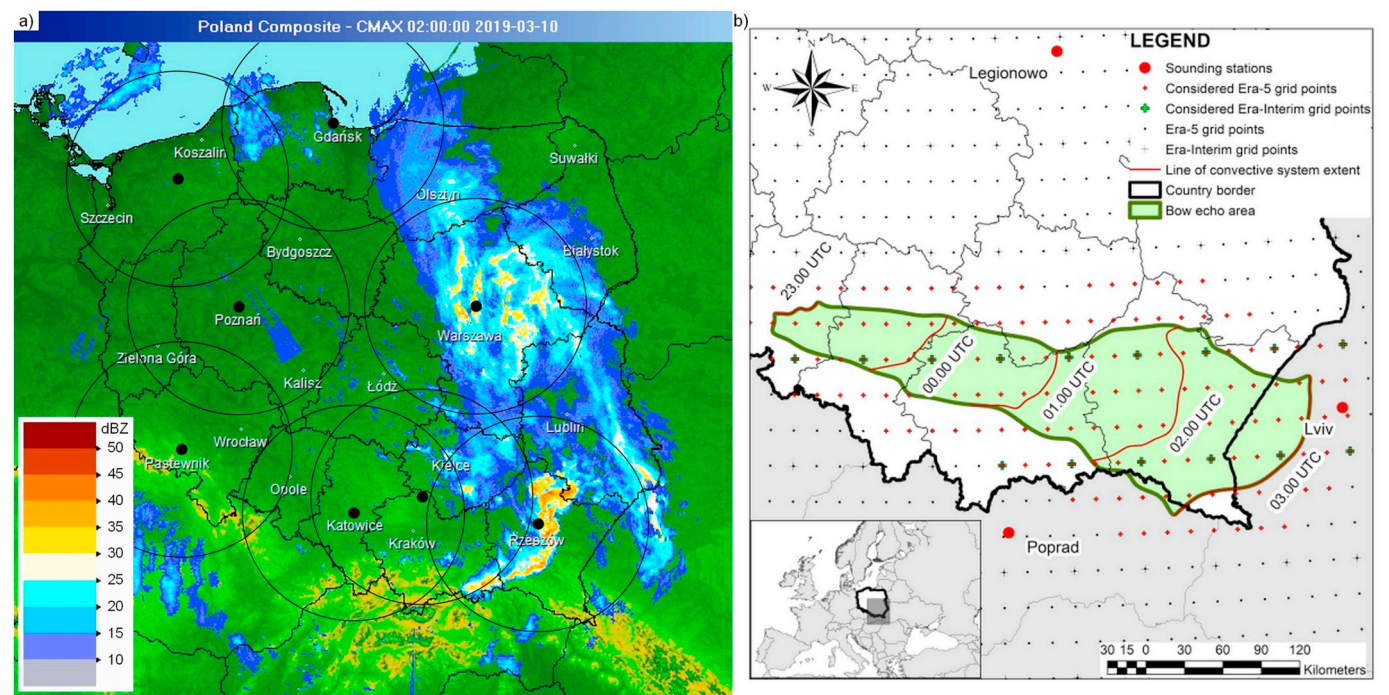


Fig. 1. A bow echo event on 09–10 March 2019: a) the radar depiction of a convective system with a bow echo — CMAX product (source: Centre for Ground Based Remote Sensing, Institute of Meteorology and Water Management – National Research Institute), along with the radars' position and 125 km circle ranges, b) the schema of the system movement along with selected grid points that were considered for this bow echo case. Note that in this case, none of the soundings met the assumed soundings selection criteria.

knmi.nl, <http://pogodynka.pl>, <http://www.wetter3.de>) with the available radar data. In the research period, we did not identify any cases that had formed within an area of wind convergence in a warm sector of a depression. According to e.g. Celiński-Mysław and Matuszko (2014) and Celiński-Mysław and Palarz (2017), such conditions support the development of bow echo, particularly in the warm season.

2.3. The atmospheric conditions

Mesoscale atmospheric conditions accompanying the bow echoes were examined based on the upper air sounding data and ERA-5 reanalysis (Hersbach et al., 2019). These conditions were defined by kinematic and thermodynamic parameters commonly used in the analysis of convective environments over Central Europe (e.g. Púčik et al., 2015; Taszarek et al., 2017)(Table 1). The Sounding and Hodograph Analysis and Research Program in Python (SHARPy—Blumberg et al., 2017) and R software (R Development Core Team, 2008) were used for calculating parameters (both for sounding and reanalysis data). Climatological distribution of 850 hPa temperature, mean sea level pressure (MSLP) and 500 hPa geopotential height, as well as their anomalies during bow echo days were determined based on data obtained from the ERA-5 reanalysis. The anomalies of monthly mean values were computed with respect to the base period of 1981–2015.

Radiosonde measurements were acquired from the atmospheric sounding database operated by the University of Wyoming (<http://weather.uwyo.edu/upperair/sounding.html>). The representative soundings for each case were selected taking into account the same criteria as in Celiński-Mysław et al. (2018). In these criteria, the proximity was defined as being within 200 km of sounding release location. In the temporal sense, in turn, a bow echo event took place up to 2 h prior to and 6 h after the sounding time. The only difference is that for CSBEs we considered soundings with any MLCAPE or MUCAPE (without minimum value of MLCAPE equal to 50 J/kg as in case of warm season cases). All zero CAPE soundings were excluded from the analysis to focus exclusively on the environments that are unstable.

Table 1
Parameters used in the study including their units and abbreviations.

Parameter	Units	Abbreviation
Moisture parameter		
Mean Mixing Ratio in the lowest 50 hPa	g/kg	MIXR
Temperature parameters		
Surface Temperature (2 m temperature)	°C	2mT
800–500 hPa temperature Lapse Rate	°C /km	tLR800–500
Parcel parameters		
Surface-Based Convective Available Potential Energy	J/kg	SBCAPE
Surface-Based Lifting Condensation Level	m	SBLLCL
50 hPa Mean Layer Convective Available Potential Energy	J/kg	MLCAPE
50 hPa Mean Layer Lifting Condensation Level	m	MLLCL
Most Unstable Convective Available Potential Energy	J/kg	MUCAPE
Most Unstable Lifting Condensation Level	m	MULCL
Downdraft Convective Available Potential Energy	J/kg	DCAPE
Kinematic parameters		
0–1 km vertical wind shear (low-level shear)	m/s	LLS
0–3 km vertical wind shear (mid-level shear)	m/s	MLS
0–6 km vertical wind shear (deep-layer shear)	m/s	DLS
The presence of the upper jet (wind speed ≥ 30 m/s in the 400–200 hPa layer)	–	Upper Jet
The presence of the lower jet (wind speed ≥ 20 m/s in the 800–500 hPa layer)	–	Lower Jet

Removal of zero CAPE profiles in proximity-sounding analysis was also applied by Rasmussen and Blanchard (1998), Brooks (2009) and Taszarek et al. (2017). Applying these criteria, the upper air analyses were limited to 21 out of possible 27 bow echo cases. Two or three representative soundings were found for 5 out of 21 cases. Consequently, we examined the values of the parameters for 27 soundings. We calculated the median values of selected parameters for all soundings. For post-frontal bow echoes, we made every effort to ensure that pre-frontal soundings were not used.

Taking into account the limitations of sounding-derived data (sparse observation network and low temporal resolution), data obtained from

ERA-5 reanalysis were also applied. The temporal resolution of the ERA-5 is 1 h, while the spatial resolution is $0.25^\circ \times 0.25^\circ$. In case of the reanalysis dataset, the research domain extends from 48° to 55.5° N and from 12° to 24.75° E. In order to compute the parameters, data from both pressure and model levels was used. Similarly as in Celiński-Mysław et al. (2018), kinematic and thermodynamic parameters were considered for each grid point located within the bow echo area and close to this area (neighboring grid points – up to 40 km from bow echo area) (Fig. 1). The closest reanalysis output time was always selected for describing the conditions of bow echo occurrence. Likewise also, we assumed that the development of a bow echo is mostly influenced by the highest shear and CAPE values, thus the grid point with the maximum parameter magnitude (one value from all grid points located within or close to the bow echo area) was established to describe the environmental conditions associated with the identified case. Other thermodynamic indices, such as MLCAPE, MUCAPE, and DCAPE were determined exactly for these grid points and time with maximum SBCAPE. To preliminarily evaluate the reanalysis dataset, we compared parameters obtained from selected sounding and the nearest ERA5 grid point (Table 2). This approach to the evaluation of reanalyses was used previously by, for example, Gensini et al. (2014), Celiński-Mysław et al. (2018) and Taszarek et al. (2018). However, owing to the restricted number of selected soundings the results must be approached with caution.

2.4. Limitations

The present study is limited in certain aspects, most importantly in terms of rather low number of analyzed cases and a quite short follow-up period (13 years). Secondly, the spatial distribution of sounding stations and the resolution of the reanalysis (especially for small-size and short-live cases) may not be sufficient to resolve the immediate environment of bow echo thunderstorms. Thirdly, although the reanalysis, in theory, represent the actual state of the atmosphere, there may be deviations from the real observations (e.g. Grünwald and Brooks, 2011; Allen and Karoly, 2014; Gensini et al., 2014; Taszarek et al., 2018), particularly in the case of thermodynamic parameters. Lastly, the identification of radar reflectivity patterns through subjective analysis (e.g. Gallus et al., 2008; Gatzen, 2011; Clark, 2013; Mulder and Schultz, 2015) may limit the amount of data that can be processed in an acceptable amount of time and is “open to judgment” of those making the manual analyses (Corfidi et al., 2016). However, these manually labeled features/signatures extracted from radar images can be utilized in future work with a machine-learning approach allowing later automatic identification (Haberlie and Ashley, 2018; Czernecki et al., 2019). In addition, certain limitations are associated also with the arbitrary division into two seasons: the cool season including cases from October to March, and the warm season from April to September. The cases that developed in October in stronger CAPE environments, are essentially more comparable with warm season bow echoes than with cool season bow echoes. The cases from April, in turn, formed generally in low CAPE conditions (Celiński-Mysław et al., 2018) which are recognizable for cool season severe wind events. Therefore, it is worth considering an extension of the cool season into April (as in Burke and Schultz, 2004) and not analyzing cases with increased CAPE from October together with other CSBEs. Although this research is confined in time and space and has some other limitations, the authors believe that

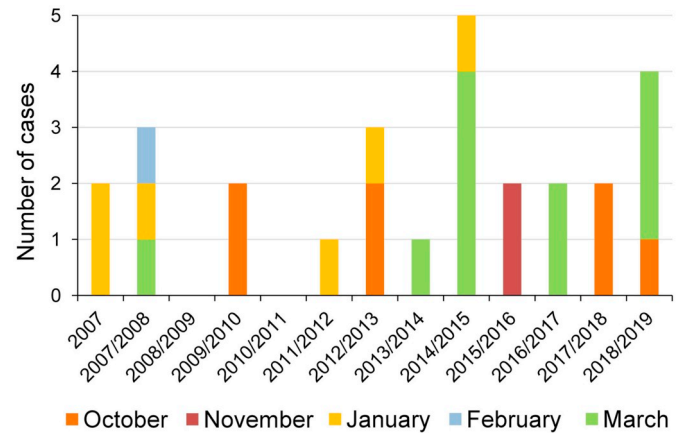


Fig. 2. The temporal distribution of the number of bow echo cases in Poland in the cool season in the years 2007–2019. Note that “2007” refers to the cases that occurred between January and March 2007, “2007/2008” to the cases that occurred between October 2007 and March 2008, and so on.

the results could be generalized to other parts of Central Europe, but cannot be certain that the findings are valid in other regions of the continent.

3. Results

In the period considered, 27 convective systems with a bow echo were identified. The most active season was 2014/2015 when 5 cases occurred. In seasons 2008/2009 and 2010/2011, CSBEs were not identified (Fig. 2).

3.1. The spatial and temporal distribution of CSBEs

Spatial extent of individual CSBEs made it possible to identify parts of the country in which their occurrence was most likely. The areas most exposed to the occurrence of CSBEs include the northern part of the Silesia province (up to 9 cases in this region), the north-western part of the Malopolska province and the central part of Wielkopolska province (Fig. 3). The northern part of Silesia province is characterized by the highest frequency of bow echo occurrence both during the cool and warm seasons (Celiński-Mysław and Palarz, 2017). The temporal distribution indicated that the highest number of CSBEs occurred in March and October. From the multi-annual perspective, 11 and 7 cases occurred in those months, respectively. In the analyzed period, 6 cases of CSBE were also found in January, 2 in November, and 1 in February (Fig. 3).

Compared to the warm season cases (Celiński-Mysław and Palarz, 2017), CSBEs were less frequent and covered mainly western and southern Poland. During the studied period, the whole area of north-eastern Poland and a large part of eastern Poland were free from their occurrence (Fig. 3). Considering the direction of movement, convective systems with a bow echo traveled predominantly from the north-west and west into the south-east and east (not shown). For a point of comparison, the western and southern directions were most frequent among warm season cases (Celiński-Mysław and Palarz, 2017).

CSBEs did not indicate as clear diurnal cycle as in warm season

Table 2

Average differences between upper air and reanalysis dataset (solely for soundings that were selected for identified bow echo cases). We used grid point nearest to the station coordinates.

Mean errors	MIXR [g/kg]	tLR800–500 [°C /km]	MLCAPE [J/kg]	SBCAPE [J/kg]	MUCAPE [J/kg]	LLS [m/s]	MLS [m/s]	DLS [m/s]
ERA-5	0.53	0.13	-6	-21	-45	-0.34	-2.18	-0.75

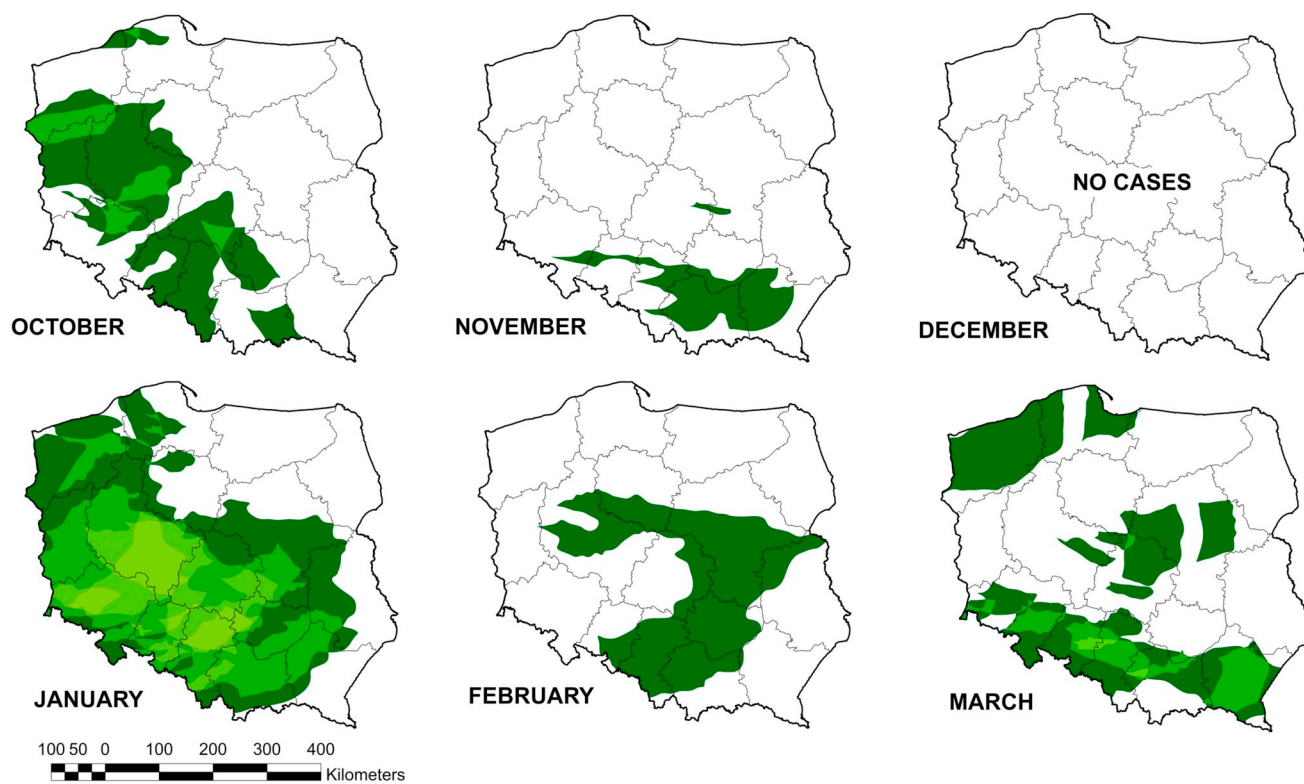
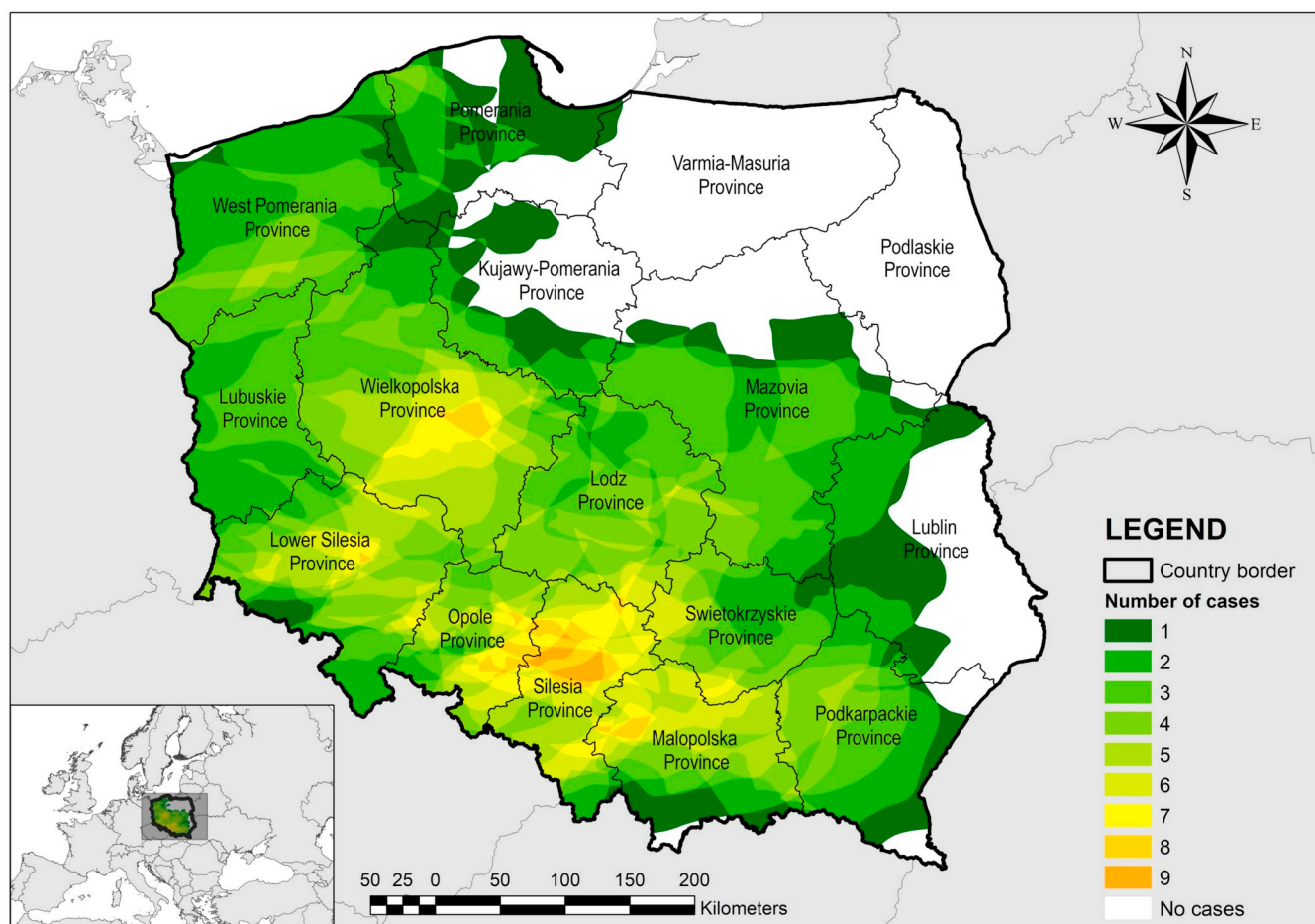


Fig. 3. The areas of bow echo occurrences in Poland (the total number of bow echo cases is a result of the overlapping of individual bow echo ranges).

Table 3

The total number of bow echo cases and their types during cool and warm season.

Season	Period	Number of cases	Type				
			BE	BEC	SLBE	CBE	DBE
Cool season	2007–2019	27	5 (19%)	7 (26%)	13 (48%)	2 (7%)	– (–)
Warm season (adapted from Celiński-Mysław and Palarz, 2017)	2007–2014	91	29 (32%)	43 (47%)	6 (7%)	4 (4%)	9 (10%)

cases when the highest frequency peaks between 15.00 and 18.00 UTC (Celiński-Mysław and Palarz, 2017). The identified cases occurred, both at day- and at night-time indicating that surface heating did not play a dominant role in CSBE formation. This is in line with the dominance of frontal events, which usually occur in strong forcing environments, largely independently of surface heating (see further).

Squall line bow echo was the predominant type of bow echo in the research period (13 out of 27 cases). Other types occurred much less frequently, i.e. BEC - 7, BE - 5, and CBE - 2. As shown in our previous study, this type occurs in Poland only in the peak of the warm season (June, July, and August). During the warm season, in turn, BECs and BEs dominated (Celiński-Mysław and Palarz, 2017)(Table 3). Taking into account the modes of bow echo developments, similarly, as in the case of warm season (Celiński-Mysław and Palarz, 2017), CSBEs developed mainly as a result of squall line transformation (15 cases) or the evolution of often weakly organized convective cells (9 cases). The remaining 3 cases formed from single storm cells.

Considering the environment of bow echo development, most cases were associated with convective systems which had developed within frontal zones of depressions. The immense majority of these were associated with cold fronts (15 cases) and just one case occurred along the articulated atmospheric front (frontal wave) with a secondary active low pressure system and one within occluded front. The remaining 10 cases formed within colder air masses to the rear of frontal systems (post-frontal cases - usually associated with surface pressure trough) (Table 4).

3.2. Synoptic patterns associated with CSBE

During the bow echo days, we observed significant negative MSLP and 500 hPa geopotential height anomalies (troughs) over northern and north-eastern Europe and strong positive anomalies (ridges) covering

Table 4

Environment of bow echo development.

Season	Environment of development (number of cases)				
	Cold front	Post-frontal convergence	Pre-frontal convergence	Articulated front/Active secondary depression	Other
Cool season	15 (55%)	10 (37%)	– (–)	1 (4%)	1 (4%)
Warm season (adapted from Celiński-Mysław and Palarz, 2017)	7 (8%)	– (–)	46 (51%)	25 (27%)	13 (14%)

the western and south-western part of the continent (Fig. 4). The analysis of 500 hPa geopotential height fields revealed identifiable troughs (often with embedded smaller-amplitude waves) moving over Poland and Central Europe in 26 out of 27 cases (in Clark, 2013 84% of cool season convective lines were associated with troughs). The cold advection on the western flank of the trough augmented the horizontal temperature gradient. The jet stream, which developed along the boundary of these thermally diverse air masses, contributed to the increase in the values of vertical wind shears (see further) providing good support for storm organization. Additionally, the areas of negative anomalies in 500 hPa geopotential height denote average tracks of synoptic lows in days with bow echo in Poland. Insofar as the average trails of synoptic depressions (base period 1981–2015) run north of the British Isles towards the middle and northern part of Scandinavia Peninsula, during the bow echo days this path is usually displaced to the south in the direction of Baltic countries and east-central Europe (not shown in the paper).

Negative geopotential anomaly and reduced activity of the semi-permanent Siberian High over eastern and northern Europe (lack of strong blocking in that region) influenced the increase of air temperature during the bow echo days. The positive 850 hPa temperature anomalies over southern and central Poland (where most of the cases were identified) reached 5 °C – highest in January (Fig. 4). The areas extending southward from Poland experienced temperature anomalies at 850 hPa exceeding even 9 °C. The 850 hPa temperature distribution that may generally be considered to be a proxy/reflection for surface temperature suggests access to warm, moist and weakly unstable air masses before the convective systems with a bow echo (particularly for the frontal cases), generally from south-western directions.

3.3. Thermodynamic conditions

It is widely known that organized deep convection, in both the warm and cool seasons, requires four main ingredients i.e. a sufficient amount of moisture in the boundary layer, a sufficiently steep lapse rate in the low and middle troposphere, a lifting mechanism to initiate and sustain convection, and strong vertical wind shear that is crucial for storm organization (e.g. Weisman and Klemp, 1982; Johns and Doswell III, 1992; Doswell III et al., 1996; Doswell III and Evans, 2003; Kuchera and Parker, 2006; to name a few). To characterize the low-level moisture during the bow echo days, we used the mean mixing ratio in the lowest 50 hPa (MIXR). As expected, the values were substantially lower than in the case of warm season bow echoes (Celiński-Mysław et al., 2018). The median value of this parameter for CSBEs exceeded 5.9 g/kg in the case of the sounding data and reached 6.2 g/kg for the ERA-5 reanalysis (Fig. 5). The highest values of MIXR, exceeding 8.5 g/kg, were found for two cases that occurred in October. The research conducted by Kolendowicz et al. (2017) for Central Europe indicated slightly lower mean/median values from soundings associated with all detected thunderstorms in the cool season.

In order to characterize vertical temperature gradient, the 800–500 hPa temperature lapse rate (tLR800–500) was used. An analysis of CSBEs indicated that the median of tLR800–500 was quite clearly higher for reanalysis data and equal to around 6.9 °C/km (Fig. 5). This is consistent with the results provided by Burke and Schultz (2004) for the cool season bow echoes in the United States (mean tLR800–500 around 7.0 °C/km for all synoptic patterns). For the sounding data, in turn, the median of tLR800–500 was equal to 6.0 °C/km. Irrespective of the dataset applied, the slightly higher values were observed for post-frontal cases (in case of ERA-5 mean tLR800–500 for post-frontal cases exceeded 7.0 °C/km). In comparison to climatological background provided by Taszarek et al. (2018), both median of MIXR and tLR800–500 for bow echoes are clearly higher. As previous studies have demonstrated steep lapse rates correspond to a greater likelihood of damaging winds and tornadoes (Johns and Hirt, 1987; Godfrey et al., 2004; Parker, 2012) both through intensification of updrafts and the

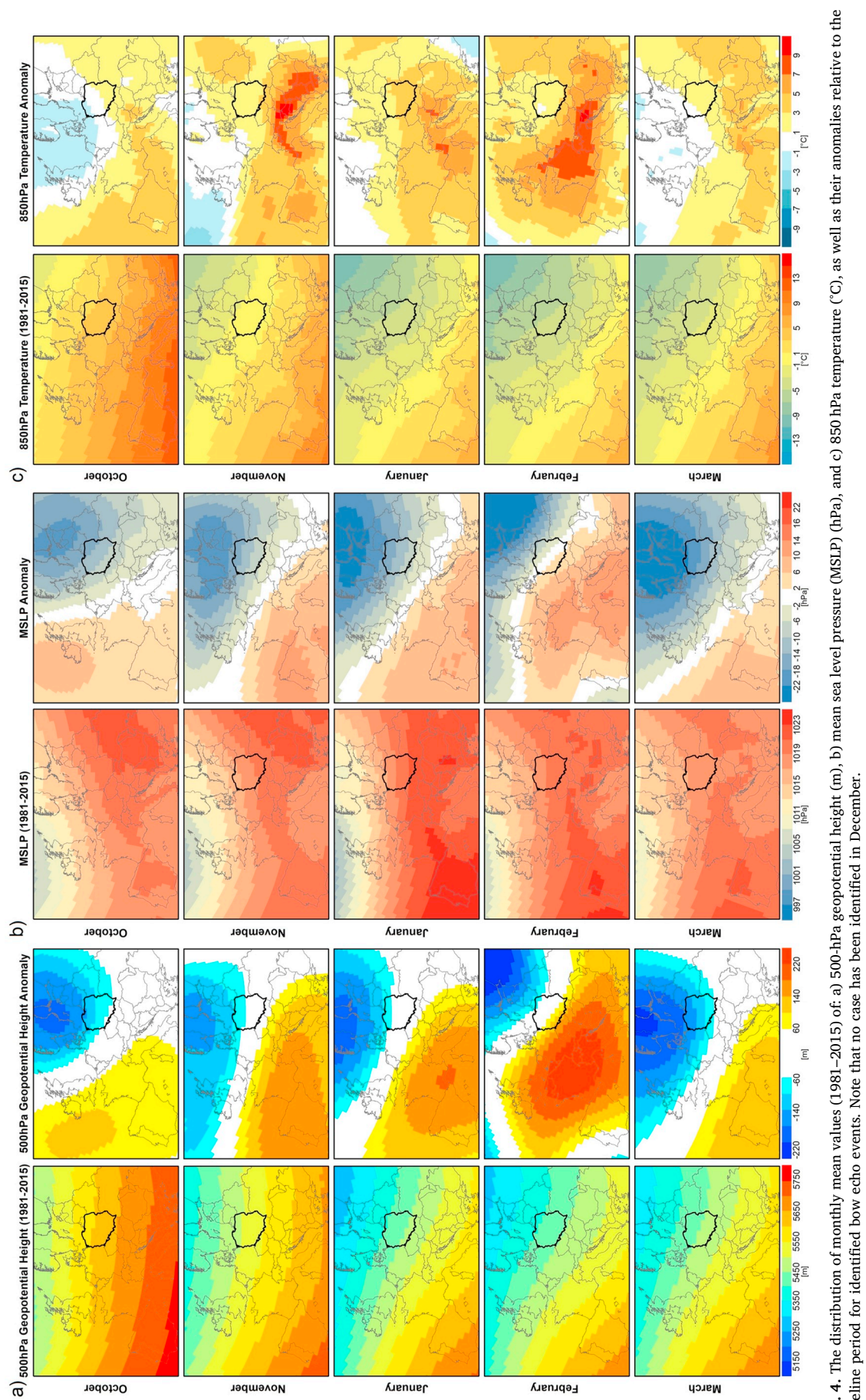


Fig. 4. The distribution of monthly mean values (1981–2015) of: a) 500-hPa geopotential height (m), b) mean sea level pressure (MSLP) (hPa), and c) 850 hPa temperature (°C), as well as their anomalies relative to the baseline period for identified bow echo events. Note that no case has been identified in December.

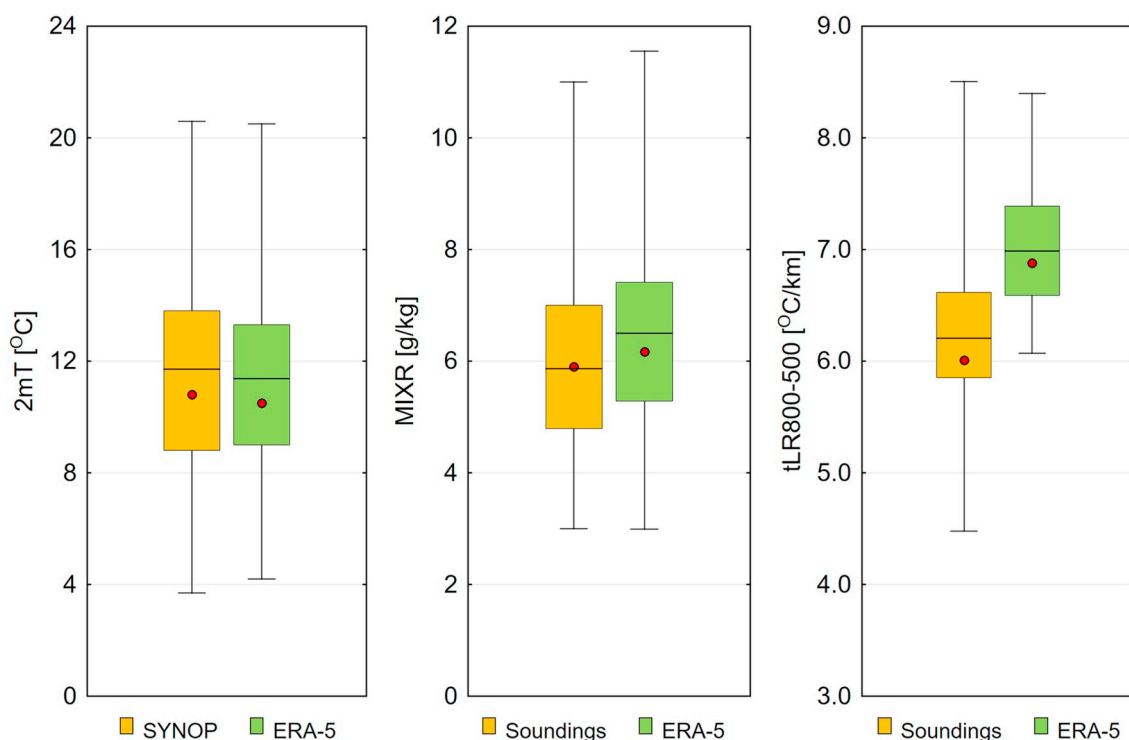


Fig. 5. Box-and-whisker plots of the range of 2mT, MIXR, and tLR800–500 associated with CSBEs. Boxes indicate the interquartile range, while whiskers mark minimum and maximum values. The median is displayed as a dot, while the mean is indicated by a central solid line through the boxes.

facilitation of downward momentum transfer. When it comes to lifting condensation level (LCL), the median value varied from 684 m (SBLCL) to 807 m (MLLCL) for soundings and from 427 (SBLCL) to 602 m (MLLCL) for ERA-5.

During CSBE days we also observed increased air temperature at 2 m height as a reflection of positive 850 hPa temperature anomalies (Fig. 4). As shown by synoptic station observations, ahead of a convective system with a bow echo, 2 m temperature (2mT) was usually substantially higher even with respect to the monthly average maximum temperature at synoptic stations (base period - 1981-2015) (not shown). For 5 cases the maximum 2mT exceeded even 15 °C (3 cases from October, 1 from November, 1 from January). Mean and median values for synoptic station observations and for ERA-5 were quite similar and were equal to around 11.5 °C (mean) and 10.6 °C (median) (Fig. 5).

The combination of steep mid-tropospheric lapse rates, low-to-moderate boundary layer moisture, and significantly lower air temperature at 2 m (compared to the warm season), resulted in low to moderate CAPE values. Higher CAPE values were observed for the re-analysis dataset. The median of SBCAPE was equal to 25 J/kg (MLCAPE = 10 J/kg, MUCAPE = 32 J/kg) for soundings, to 127 J/kg (MLCAPE = 100 J/kg, MUCAPE = 135 J/kg) for ERA-5. However, the maximum MUCAPE values exceeded even 500 J/kg (Fig. 6). In contrast to shear parameters (see further), the higher values of CAPE indices were usually revealed for post-frontal cases (regardless of the dataset).

As discussed in Celiński-Mysław et al. (2018), the increased values of CAPE and DCAPE (in comparison to the values for severe wind events demonstrated by Púčik et al. (2015) for Central Europe) were usually necessary for bow echo formation in the warm season. This was particularly important for the cases associated with convective systems that had developed in weakly forced environments. The cool season cases, in turn, are driven by strong synoptic-scale lift (bow echo usually on the eastern flank of a well-pronounced trough, i.e. in the zone of upper-level divergence) and fast mean flow (see further), compensating in this way usually low CAPE and low DCAPE. The median DCAPE for CSBEs reached 208 J/kg for soundings and 173 J/kg for ERA-5 (Fig. 7). Thus,

according to the results obtained, high values of DCAPE are not necessary for enhancing the risk of wind damage during the cool season. This is in line with the research performed by Púčik et al. (2015) who showed that for cool season severe wind gust events in Central Europe, the magnitude of DCAPE is usually very low (median DCAPE equal to 79 J/kg).

3.4. Kinematic conditions

The CSBEs were always associated with the presence of strong air flow in the troposphere. Bearing in mind the assumed thresholds (Table 1) (the same as in Celiński-Mysław et al., 2018 – Upper Jet > 30 m/s, Lower Jet > 20 m/s) jet streams on different levels were observed for all identified bow echo cases. The maximum wind speed within the upper jet achieved more than 70 m/s (for 2 cases). At 500 hPa, in turn, the lower jet stream attained a horizontal speed of more than 50 m/s (for 3 cases). The analysis conducted also revealed that the post-frontal cases were accompanied by a lower wind speed both within the upper and lower jet (based on ERA-5). The mean value for frontal cases was approximately equal to 54.6 m/s in the case of upper jet and 39.0 m/s in the case of lower jet, while the mean maximum value for post-frontal cases was around 47.0 m/s for upper jet and 35.5 m/s for the lower jet.

Considerably increased values for vertical wind shear are generally a direct consequence of strong air flow in the middle and upper troposphere. The wind shear that are crucial for spatial arrangement, the maximum size and longevity of convective systems (e.g. Weisman and Klemp, 1982; Evans and Doswell III, 2001; Burke and Schultz, 2004) achieved here frequently very large values. The CSBEs formed in an environment with DLS well above 50 m/s (–2 cases for ERA-5), with MLS exceeded 40 m/s (–1 case for ERA-5), and with LLS up to 29.9 m/s (ERA-5). The median value of vertical wind shears for identified cases exceeded 30 m/s for DLS (30.5 m/s for soundings; 34.6 m/s for ERA-5), was well above 20 m/s for MLS (24.5 m/s for soundings; 24.3 m/s for ERA-5) and higher than 18 m/s for LLS (18.2 m/s for soundings; 21.0 m/s for ERA-5). Wherein, the significantly higher values of shear

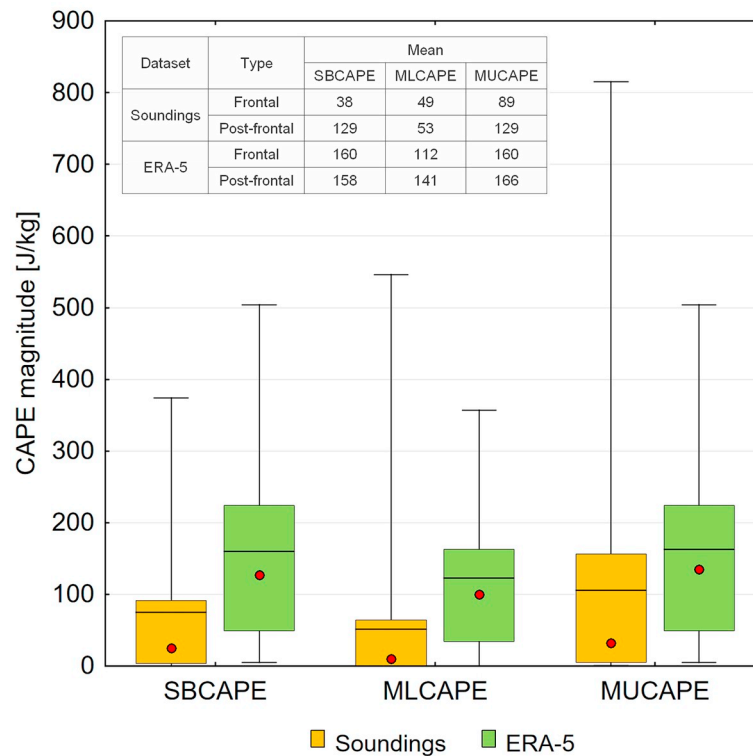


Fig. 6. As in Fig. 5, but for SBCAPE, MLCAPE, and MUCAPE.

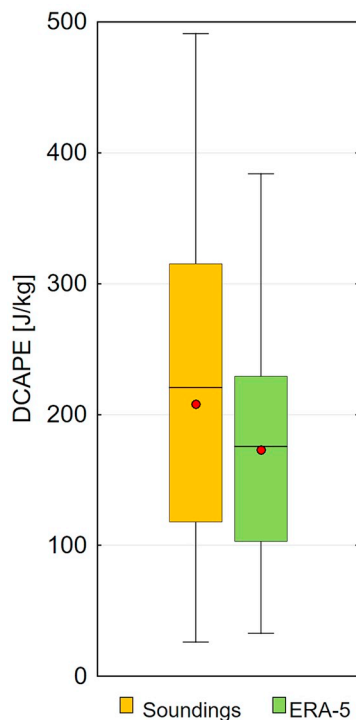


Fig. 7. As in Fig. 5, but for DCAPE.

parameters are characteristic for frontal cases (Fig. 8) – conversely for CAPE (higher values for post-frontal case). Our results show also that the median values of shear parameters for bow echoes are significantly higher than climatological background presented in Taszarek et al. (2018). As they demonstrated, the median of DLS for Central Europe and Balkans varied from around 15.0 m/s in October and March to around 18.0 m/s in January, while the median of LLS did not exceed

7.5 m/s in any cool season month.

4. Discussion

Although the activity of mesoscale convective systems is least common during the cool season, significant wind events (such as bow echo and derecho) do happen over Central and Western Europe every year (e.g. Fink et al., 2009; Gatzen et al., 2011; Celiński-Mysław and Matuszko, 2014; Gatzen et al., 2019; Mathias et al., 2019). To improve our understanding of CSBEs, this study has established a climatology of such events, providing also an insight into the atmospheric conditions accompanying identified cases. During the period studied, 27 cool season bow echoes were identified across Poland, which stands in contrast to the 91 warm season cases recognized between 2007 and 2014 (Celiński-Mysław and Palarz, 2017). Given the fact that diurnal heating is limited during the cool season, the lack of a clear 24-h cycle of CSBE occurrence seems natural. This is consistent with the findings of, for example, Bentley and Mote (1998) for cool season derecho events in the United States; Gatzen et al. (2011) for cool season narrow cold-frontal rainbands in Germany; Clark (2013) for cool season convective lines in the UK; and Gatzen et al. (2019) for cool season derechos in Germany. On the other hand, many studies have demonstrated that the highest frequency of severe thunderstorms during the warm season peaks in the afternoon (e.g. Groenemeijer and Kühne, 2014; Taszarek and Brooks, 2015; Celiński-Mysław and Palarz, 2017).

Comparing types of bow echo between warm and cool seasons, it could be noted that the predominant types in the warm half of the year included BEC and BE (72 out of 91 cases – Celiński-Mysław and Palarz, 2017), while SLBE in the cool season (13 out of 27 – this article). Considering the synoptic-scale environment of bow echo development, in turn, CSBEs were mostly associated with cold frontal zones, while most warm season cases developed within convergence zones in the warm sector of depression or within an articulated atmospheric front with a secondary active low-pressure system (Celiński-Mysław and Palarz, 2017). The research reported here also demonstrated a

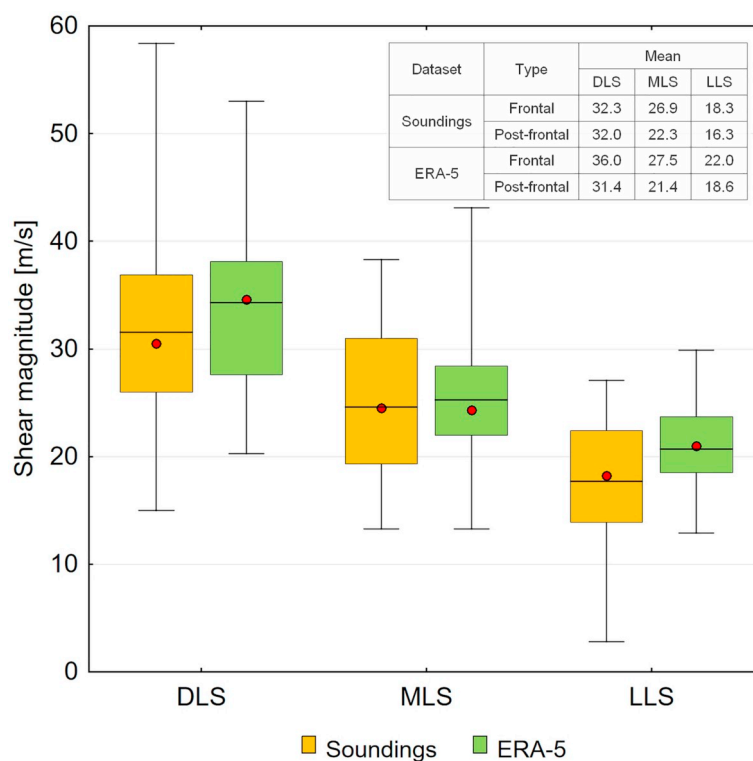


Fig. 8. As in Fig. 5, but for DLS, MLS, and LLS.

significant share of post-frontal cases in the total number of CSBEs. As indicated in the study provided by Clark (2013), 13% of cool season convective lines in the UK occurred exactly in post-frontal situations. Also, for example, the case of the cool season derecho from western Europe on 3 January 2014, analyzed by Mathias et al. (2019), was related to a surface pressure trough in a post-frontal air masses.

Our research showed that, in the cool season, the pre-storm environment is predominantly characterized by weak instability (small or negligible CAPE) and strong vertical wind shear. These high shear/low CAPE environments in combination with triggering mechanism along the front (frontal cases) or along the surface trough (post-frontal cases) can be considered as supportive for the formation of bow echoes. This is consistent with the findings of, for example, Mathias et al. (2019), who performed hindcast experiments of a cool season derecho in Western Europe. As previous studies have shown, strong, large-scale convergence and lift provided by the mid-latitude depressions with active fronts foster a deep convection effect during the cool season even in low-CAPE environments (e.g. Jewett and Wilhelmson, 2006; Gatzen, 2011; Clark, 2013; Celiński-Mysław and Matuszko, 2014). It can therefore be concluded, that cool season bow echo events are usually supported by a strong synoptic-scale lift over Central Europe. As demonstrated by this study, the bow echo thunderstorm formation was strongly affected by the presence of fast flow from mid to upper level. The jet streams on different levels were observed for all identified CSBEs. According to Clark's (2013) research, most of the cool season convective lines occur under jet core or close to the exit region of the jet (for the UK area). The presence of the jet stream contributes to the increase in vertical wind shear values. The higher values of vertical wind shears, in turn, support spatial arrangement/organization of the convective system (e.g. bow echo), affect its maximum size and intensity, and as well are conducive its longevity (e.g. Rotunno et al., 1988; Johns, 1993; Weisman, 1993; Evans and Doswell III, 2001; Cohen et al., 2007; Brooks, 2009; Púčik et al., 2015). The median values of shear parameters here are generally in the range of the values found by Púčik et al. (2015) for cool season severe wind gust events in Central Europe, but are clearly stronger compared with the shear values

(0–2.5 km shear and 0–5.0 km shear) identified by Burke and Schultz (2004) for cool season bow echoes over the continental United States. It is worth pointing out, however, that the cool season in Burke's and Schultz's (2004) research had been extended to the end of April (18 out of 51 cases occurred exactly in April), and CAPE values for their cases were markedly higher compared with those for Poland. As shown in the prior studies, regardless of the season, a significantly higher instability over the United States than over Europe was identified for severe wind events (Klimowski et al., 2004; Kuchera and Parker, 2006; Grünwald and Brooks, 2011; Púčik et al., 2015; Taszarek et al., 2017; Celiński-Mysław et al., 2018). The median of shear values for CSBEs are also slightly higher than in Clark (2013) in comparison to both tornadic and non-tornadic cool season convective lines in the UK. Our results show also that post-frontal cases form generally in the environment with weaker shear and higher CAPE in comparison with those associated with the cold front. This is consistent with the findings of Mathias et al. (2019), who compared the shear values accompanying the cool season derecho that occurred on 3 January 2014 in Western Europe (post-frontal case – weaker shears) with the cases analyzed by Gatzen et al. (2011) formed along a cold front (stronger shears). Furthermore, it is worth adding that cool season bow echoes occur in environments of very weak instability, but generally not as weak as cold-season narrow cold-frontal rainbands in Germany (Gatzen, 2011 – mean MLCAPE = 13 J/kg).

The study has also demonstrated generally higher values of all the CAPE (MLCAPE, SBCAPE, MUCAPE) and shear parameters (DLS, MLS, LLS) (Table 2) for selected soundings comparing with the nearest ERA-5 grid points. However, it should be emphasized that the differences (particularly in CAPE values) for some cases were quite large and this could significantly influence the average values. Based on the previous works (e.g. Coniglio, 2012; Allen and Karoly, 2014; Gensini et al., 2014; Taszarek et al., 2018), it is apparent that CAPE fields from model/re-analysis datasets may be inaccurate owing to errors particularly in low-level moisture content, boundary layer height, or lapse rates. So, as mentioned before, owing to the limited number of selected soundings, mean differences in CAPE values should be approached with caution. In

case of shear parameters, the highest differences occurred in MLS values. As many previous studies have shown (e.g. Weisman and Trapp, 2003; Atkins and St Laurent, 2009; Taszarek et al., 2017, 2019; Celiński-Mysław et al., 2018), high values of this parameter are considered as particularly conducive to the development of convective systems with damaging wind potential (e.g. bow echo and derecho). The underestimation of the shear parameters in the reanalysis datasets has been previously found by, for example, Brooks et al. (2003), Allen et al. (2011), Celiński-Mysław et al. (2018) and Taszarek et al. (2018). Additionally, fairly small mean differences in the shear parameters between soundings and ERA-5 reanalysis may support previous findings which suggested that kinematic parameters are better represented in contrast to thermodynamic indices (e.g. Allen and Karoly, 2014; Gensini et al., 2014; Taszarek et al., 2018).

5. Conclusions

The goal of this study was to determine the spatiotemporal distribution of cool season bow echoes in Poland, and to present the atmospheric conditions associated with such events. During the period studied (January 2007 and March 2019), 27 convective systems with a bow echo over Poland have been identified. Important findings are listed below:

- The area most exposed to the occurrence of CSBEs included south-western Poland, while the north-eastern and eastern part of the country was generally free from this phenomenon.
- CSBEs do not indicate a clear diurnal cycle (unlike the warm season cases).
- The predominant types in the cool half of the year included SLBE, while BEC and BE were included in the warm season (Celiński-Mysław and Palarz, 2017).
- The immense majority of CSBEs (25 out of 27 cases) formed within cold frontal zones or within surface pressure troughs in postfrontal air masses.
- The analysis of 500 hPa geopotential height fields revealed identifiable troughs (often with embedded smaller-amplitude dynamic waves) moving over Poland and Central Europe in 26 out of 27 cases.
- During bow echo days, we observed significant negative MSLP and 500 hPa geopotential height anomalies over northern and north-eastern Europe and strong positive anomalies covering the western and south-western parts of the continent.
- According to the results obtained, cool season bow echo storm formation is strongly affected by the presence of fast flow from mid to upper level. The jet streams on different levels were observed for all identified CSBEs.
- In the cool season, the bow echo environment is predominantly characterized by weak instability and strong vertical wind shear (strongly forced synoptic regime).
- A recurring finding was that post-frontal cases formed in an environment with weaker shear, but higher CAPE.

In summary, the results here provide a baseline that can help forecasters anticipate the risk of bow echo storms in the cool season, especially in a given location. However, additional observational and numerical studies about cool season bow echoes are needed to better understand the processes responsible for their development and to better recognize atmospheric conditions accompanying these phenomena.

Declaration of Competing Interest

None.

Acknowledgements

This study was possible thanks to research grants from Jagiellonian University (project number: K/DSC/005467) and National Science Centre (project number: 2017/27/B/ST10/00297). Authors also greatly appreciate the support from the Polish Institute of Meteorology and Water Management – National Research Institute for providing radar data and the ECMWF for providing the ERA5 reanalysis.

References

- Adams-Selin, R.D., Johnson, R.H., 2010. Mesoscale surface pressure and temperature features associated with bow echoes. *Mon. Weather Rev.* 138, 212–227. <https://doi.org/10.1175/2009MWR2892.1>.
- Allen, J.T., Karoly, D.J., 2014. A climatology of Australian severe thunderstorm environments 1979–2011: inter-annual variability and ENSO influence. *Int. J. Climatol.* 34, 81–97. <https://doi.org/10.1002/joc.3667>.
- Atkins, N.T., St Laurent, M., 2009. Bow echo mesovortices. Part I: processes that influence their damaging potential. *Mon. Weather Rev.* 137, 1497–1513. <https://doi.org/10.1175/2008MWR2649.1>.
- Bentley, M.L., Mote, T.L., 1998. A climatology of derecho producing mesoscale convective systems in the central and eastern United States, 1986–95 Part I: temporal and spatial distribution. *Bull. Am. Meteorol. Soc.* 79, 2527–2540. [https://doi.org/10.1175/1520-0477\(1998\)079<2527:ACODPM>2.0.CO;2](https://doi.org/10.1175/1520-0477(1998)079<2527:ACODPM>2.0.CO;2).
- Blumberg, W.G., Halbert, K.T., Supinie, T.A., Marsh, P.T., Thompson, R.L., Hart, J.A., 2017. SHARPPy: an open-source sounding analysis toolkit for the atmospheric sciences. *Bull. Am. Meteorol. Soc.* 98, 1625–1636. <https://doi.org/10.1175/BAMS-D-15-00309.1>.
- Brooks, H.E., 2009. Proximity soundings for severe convection for Europe and the United States from reanalysis data. *Atmos. Res.* 93, 546–553. <https://doi.org/10.1016/j.atmosres.2008.10.005>.
- Brooks, H.E., Lee, J.W., Craven, J.P., 2003. The spatial distribution of severe thunderstorms and tornado environments from global reanalysis data. *Atmos. Res.* 67–68, 73–94. [https://doi.org/10.1016/S0169-8095\(03\)00045-0](https://doi.org/10.1016/S0169-8095(03)00045-0).
- Burke, P.C., Schultz, D.M., 2004. A 4-Yr Climatology of Cold-Season Bow Echoes over the Continental United States. *Wea. Forecasting* 19, 1061–1074. <https://doi.org/10.1175/811.1>.
- Celiński-Mysław, D., Matuszko, D., 2014. An analysis of the selected cases of derecho in Poland. *Atmos. Res.* 149, 263–281. <https://doi.org/10.1016/j.atmosres.2014.06.016>.
- Celiński-Mysław, D., Palarz, A., 2017. The occurrence of convective systems with a bow echo in warm season in Poland. *Atmos. Res.* 193, 26–35. <https://doi.org/10.1016/j.atmosres.2017.04.015>.
- Celiński-Mysław, D., Palarz, A., Łoboda, Ł., 2018. Kinematic and thermodynamic conditions related to convective systems with a bow echo in Poland. *Theor. Appl. Climatol.* 137 (2109), 1–11. <https://doi.org/10.1007/s00704-018-2728-6>.
- Clark, M.R., 2009. The southern England tornadoes of 30 December 2006: case study of a tornadic storm in a low CAPE, high shear environment. *Atmos. Res.* 93, 50–65. <https://doi.org/10.1016/j.atmosres.2008.10.008>.
- Clark, M.R., 2013. A provisional climatology of cool-season convective lines in the UK. *Atmos. Res.* 123, 180–196. <https://doi.org/10.1016/j.atmosres.2012.09.018>.
- Cohen, A.E., Coniglio, M.C., Corfidi, S.F., Corfidi, S.J., 2007. Discrimination of mesoscale convective system environments using sounding observations. *Wea. Forecasting* 22, 1045–1062. <https://doi.org/10.1175/WAF1040.1>.
- Coniglio, M.C., 2012. Verification of RUC0–1-h forecasts and SPC mesoscale analyses using VORTEX2 soundings. *Wea. Forecasting* 27, 667–683. <https://doi.org/10.1175/WAF-D-11-00096.1>.
- Corfidi, S.F., Coniglio, M.C., Cohen, A.E., Mead, C.M., 2016. A proposed revision to the definition of “derecho”. *Bull. Amer. Meteor. Soc.* 97, 935–949. <https://doi.org/10.1175/BAMS-D-14-00254.1>.
- Czernecki, B., Taszarek, M., Marosz, M., Pórolniczak, M., Kolendowicz, L., Wyszogrodzki, A., Szturc, J., 2019. Application of machine learning to large hail prediction - the importance of radar reflectivity, lightning occurrence and convective parameters derived from ERA5. *Atmos. Res.* 227, 249–262. <https://doi.org/10.1016/j.atmosres.2019.05.010>.
- Doswell III, C.A., Evans, J.S., 2003. Proximity sounding analysis for derechos and supercells: an assessment of similarities and differences. *Atmos. Res.* 67–68, 117–133. [https://doi.org/10.1016/S0169-8095\(03\)00047-4](https://doi.org/10.1016/S0169-8095(03)00047-4).
- Doswell III, C.A., Brooks, H.E., Maddox, R.A., 1996. Flash flood forecasting: an Ingredients-based Methodology. *Wea. Forecasting* 11, 560–581. [https://doi.org/10.1175/1520-0434\(1996\)011<0560:FFFAIB>2.0.CO;2](https://doi.org/10.1175/1520-0434(1996)011<0560:FFFAIB>2.0.CO;2).
- Earl, N., Dorling, S., Starks, M., Finch, R., 2017. Subsynoptic-scale features associated with extreme surface gusts in UK extratropical cyclone events. *Geophys. Res. Lett.* 44, 3932–3940. <https://doi.org/10.1002/2017GL073124>.
- Evans, J.S., Doswell III, C.A., 2001. Examination of derecho environments using proximity soundings. *Wea. Forecasting* 16, 329–342. [https://doi.org/10.1175/1520-0434\(2001\)016.0329:EODEUP.2.0.CO;2](https://doi.org/10.1175/1520-0434(2001)016.0329:EODEUP.2.0.CO;2).
- Fink, A.H., Brücher, T., Ermert, V., Krüger, A., Pinto, J.G., 2009. The European storm Kyrill in January 2007: Synoptic evolution, meteorological impacts and some considerations with respect to climate change. *Nat. Hazards Earth Syst. Sci.* 9, 405–423. <https://doi.org/10.5194/nhess-9-405-2009>.
- Fujita, T.T., 1978. Manual of downburst identification for project NIMROD. In: *Satellite & Mesometeorology Research Project*. The University of Chicago (104 pp).

- Gallus, W.A., Snook Jr., N.A., Johnson, E.V., 2008. Spring and summer severe weather reports over the Mid-west as a function of convective mode: a preliminary study. *Wea. Forecasting* 23, 101–113. <https://doi.org/10.1175/2007WAF0006120.1>.
- Gatzen, C., 2011. A 10-year climatology of cold-season narrow cold-frontal rainbands in Germany. *Atmos. Res.* 100, 366–370. <https://doi.org/10.1016/j.atmosres.2010.09.018>.
- Gatzen, C., 2013. Warm-season severe wind events in Germany. *Atmos. Res.* 123, 197–205. <https://doi.org/10.1016/j.atmosres.2012.07.017>.
- Gatzen, C., Púčik, T., Ryva, D., 2011. Two cold-season derechos in Europe. *Atmos. Res.* 100, 740–748. <https://doi.org/10.1016/j.atmosres.2010.11.015>.
- Gatzen, C., Fink, A.H., Schultz, D.M., Pinto, J.G., 2019. An 18-year climatology of derechos in Germany. *Nat. Hazards Earth Syst. Sci.* <https://doi.org/10.5194/nhess-2019-234>.
- Gensini, V.A., Mote, T.L., Brooks, H.E., 2014. Severe-thunderstorm reanalysis environments and collocated radiosonde observations. *J. Appl. Meteorol. Climatol.* 53, 742–751. <https://doi.org/10.1175/JAMC-D-13-0263.1>.
- Godfrey, E.S., Trapp, R.J., Brooks, H.E., 2004. A study of the pre-storm environment of tornadic quasi-linear convective systems. In: *Preprints, 22nd Conf. On Severe Local Storms*, Hyannis, MA, Amer. Meteor. Soc. 3A.5, [Available online at <https://ams.confex.com/ams/pdfpapers/81388.pdf>].
- Gospodinov, I., Dimitrova, T., Bocheva, L., Simeonov, P., Dimitov, R., 2015. Derecho-like event in Bulgaria on 20 July 2011. *Atmos. Res.* 158–159, 254–273. <https://doi.org/10.1016/j.atmosres.2014.05.009>.
- Groenemeijer, P., Kühne, T., 2014. A climatology of tornadoes in Europe: results from the European severe weather database. *Mon. Weather Rev.* 142, 4775–4790. <https://doi.org/10.1175/MWR-D-14-00107.1>.
- Grünwald, S., Brooks, H.E., 2011. Relationship between sounding derived parameters and the strength of tornadoes in Europe and the USA from reanalysis data. *Atmos. Res.* 100, 479–488. <https://doi.org/10.1016/j.atmosres.2010.11.011>.
- Haberlie, A.M., Ashley, W.S., 2018. A method for identifying midlatitude mesoscale convective systems in radar mosaics. Part II. Tracking. *J. Appl. Meteorol. Clim.* 57, 1599–1621. <https://doi.org/10.1175/jamc-d-17-0294.1>.
- Hersbach, H., Bell, B., Berrisford, P., Horányi, A., Muñoz Sabater, J., Nicolas, J., Radu, R., Schepers, D., Simmons, A., Soci, C., Dee, D., 2019. Global reanalysis: goodbye ERA-Interim, hello ERA5. *ECMWF Newsletter* 159, 17–24. <https://doi.org/10.21957/vf291hehd7>.
- Jewett, B.F., Wilhelmson, R.B., 2006. The role of forcing in cell morphology and evolution within midlatitude squall lines. *Mon. Weather Rev.* 134, 3714–3734. <https://doi.org/10.1175/MWR3164.1>.
- Johns, R.H., 1993. Meteorological conditions associated with bow echo development in convective storms. *Wea. Forecasting* 8, 294–299. [https://doi.org/10.1175/1520-0434\(1993\)008<0294:MCAWBE>2.0.CO;2](https://doi.org/10.1175/1520-0434(1993)008<0294:MCAWBE>2.0.CO;2).
- Johns, R.H., Doswell III, C.A., 1992. Severe local storms forecasting. *Wea. Forecasting* 7, 588–612. [https://doi.org/10.1175/1520-0434\(1992\)007<0588:SLSF.2.0.CO;2](https://doi.org/10.1175/1520-0434(1992)007<0588:SLSF.2.0.CO;2).
- Johns, R.H., Hirt, W.D., 1987. Derechos: widespread convectively induced wind storms. *Wea. Forecasting* 2, 32–49. [https://doi.org/10.1175/1520-0434\(1987\)002<0032:DWCIW>2.0.CO;2](https://doi.org/10.1175/1520-0434(1987)002<0032:DWCIW>2.0.CO;2).
- King, J.R., Parker, M., Sherburn, K.D., Lackmann, G.M., 2017. Rapid Evolution of cool season, Low-CAPE Severe Thunderstorm Environments. *Wea. Forecasting* 32, 763–779. <https://doi.org/10.1175/WAF-D-16-0141.1>.
- Klimowski, B.A., Przybylinski, R.W., Schmocker, G., Hjelmfelt, M.R., 2000. Observations of the formation and early evolution of bow echoes. In: *20th Conference on Severe Local Storms*. Amer. Meteor. Soc., Orlando, pp. 44–47. (Available online at). <http://www.crh.noaa.gov/Image/urx/soo/sels20-final.pdf>.
- Klimowski, B.A., Hjelmfelt, M.R., Bunkers, M.J., 2004. Radar observations of the early evolution of bow echoes. *Wea. Forecasting* 19, 727–734. [https://doi.org/10.1175/1520-0434\(2004\)019<0727:502:ROOTEE>2.0.CO;2](https://doi.org/10.1175/1520-0434(2004)019<0727:502:ROOTEE>2.0.CO;2).
- Kolendowicz, L., Tazarek, M., Czernecki, B., 2017. Atmospheric circulation and sounding-derived parameters associated with thunderstorm occurrence in Central Europe. *Atmos. Res.* 191, 101–114. <https://doi.org/10.1016/j.atmosres.2017.03.009>.
- Koukourou, R., Mills, G., Timbal, B., 2009. A reanalysis climatology of cool-season tornado environments over southern Australia. *Int. J. Climatol.* 29, 2079–2090. <https://doi.org/10.1002/joc.1856>.
- Kuchera, E.L., Parker, M.D., 2006. Severe convective wind environments. *Wea. Forecasting* 21, 595–612. <https://doi.org/10.1175/WAF931.1>.
- Ludwig, P., Pinto, J., Hoeppe, S., Fink, A., Gray, S., 2015. Secondary cyclogenesis along an occluded front leading to damaging wind gusts: Windstorm Kyrill, January 2007. *Mon. Weather Rev.* 143, 1417–1437. <https://doi.org/10.1175/mwr-d-14-00304.1>.
- Mathias, L., Erment, V., Kelemen, F.D., Ludwig, P., 2017. Synoptic analysis and hindcast of an intense bow echo in Western Europe: the 9 June 2014 storm. *Wea. Forecasting* 32, 1121–1141. <https://doi.org/10.1175/WAF-D-16-0192.1>.
- Mathias, L., Ludwig, P., Pinto, J.G., 2019. Synoptic-scale conditions and convection-resolving hindcast experiments of a cold-season derecho on 3 January 2014 in western Europe. *Nat. Hazards Earth Syst. Sci.* 19, 1023–1040. <https://doi.org/10.5194/nhess-19-1023-2019>.
- Mulder, K.J., Schultz, D.M., 2015. Climatology, storm morphologies, and environments of tornadoes in the British Isles: 1980–2012. *Mon. Weather Rev.* 143, 2224–2240. <https://doi.org/10.1175/MWR-D-14-00299.1>.
- Ośródk, K., Szturc, J., Jurczyk, A., 2014. Chain of data quality algorithms for 3-D single polarization radar reflectivity (RADVOL-QC system). *Meteorol. Appl.* 21, 256–270. <https://doi.org/10.1002/met.1323>.
- Parker, M.D., 2012. Impacts of lapse rates on low-level rotation in idealized storms. *J. Atmos. Sci.* 69, 538–559. <https://doi.org/10.1175/JAS-D-11-058.1>.
- Púčik, T., Francova, M., Ryva, D., Kolar, M., Ronge, L., 2011. Forecasting challenges during the severe weather outbreak in Central Europe on 25 June 2008. *Atmos. Res.* 100, 680–704. <https://doi.org/10.1016/j.atmosres.2010.11.014>.
- Púčik, T., Groenemeijer, P., Ryva, D., Kolar, M., 2015. Proximity soundings of severe and nonsevere thunderstorm in Central Europe. *Mon. Weather Rev.* 143, 4805–4821. <https://doi.org/10.1175/MWR-D-15-0104.1>.
- Punkka, A.-J., Teittinen, J., Johns, R.H., 2006. Synoptic and mesoscale analysis of a high-latitude derecho-severe thunderstorm outbreak in Finland on 5 July 2002. *Wea. Forecasting* 21, 752–763. <https://doi.org/10.1175/WAF953.1>.
- Rasmussen, E.N., Blanchard, D.O., 1998. A baseline climatology of sounding-derived supercell and tornado forecast parameters. *Wea. Forecasting* 13, 1148–1164. [https://doi.org/10.1175/1520-0434\(1998\)008<1148%3AABCSO%3E2.0.CO;2](https://doi.org/10.1175/1520-0434(1998)008<1148%3AABCSO%3E2.0.CO;2).
- R Development Core Team, 2008. R: A language and environment for statistical computing. R Foundation for Statistical Computing, Vienna, Austria. <http://www.R-project.org>.
- Rotunno, R., Klemp, J.B., Weisman, M.L., 1988. A theory for strong, long-lived squall lines. *J. Atmos. Sci.* 45, 463–485. [https://doi.org/10.1175/1520-0469\(1988\)045<0463:ATFSL>2.0.CO;2](https://doi.org/10.1175/1520-0469(1988)045<0463:ATFSL>2.0.CO;2).
- Sherburn, K.D., Parker, M.D., King, J.R., Lackmann, G.M., 2016. Composite environments of severe and nonsevere High-Shear, Low-CAPE Convective Events. *Wea. Forecasting* 31, 1899–1927. <https://doi.org/10.1175/WAF-D-16-0086.1>.
- Tazarek, M., Brooks, H.E., 2015. Tornado climatology of Poland. *Mon. Weather Rev.* 143, 702–717. <https://doi.org/10.1175/MWR-D-14-00185.1>.
- Tazarek, M., Brooks, H.E., Czernecki, B., 2017. Sounding-derived parameters associated with convective hazards in Europe. *Mon. Weather Rev.* 145, 1511–1528. <https://doi.org/10.1175/MWR-D-16-0384.1>.
- Tazarek, M., Brooks, H.E., Czernecki, B., Szuster, P., Fortuniak, K., 2018. Climatological aspects of convective parameters over Europe: a comparison of ERA-interim and sounding data. *J. Clim.* 31, 4281–4308. <https://doi.org/10.1175/JCLI-D-17-0596.1>.
- Tazarek, M., Pilgus, N., Orlikowski, J., Surowiecki, A., Walczakiewicz, S., Pilorz, W., Piasecki, K., Pajurek, L., Pórolniczak, M., 2019. Derecho evolving from a mesocyclone – a study of 11 August 2017 severe weather outbreak in Poland: event analysis and high-resolution simulation. *Mon. Wea. Rev.* In press. <https://doi.org/10.1175/MWR-D-18-0330.1>.
- Toll, V., Männik, A., Luhamaa, A., Rõm, R., 2015. Hindcast experiments of the derecho in Estonia on 8 August, 2010: Modelling derecho with NWP model HARMONIE. *Atmos. Res.* 158–159, 179–191. <https://doi.org/10.1016/j.atmosres.2014.10.011>.
- Trapp, R.J., Tessendorf, S.A., Godfrey, E.S., Brooks, H.E., 2005. Tornadoes from squall lines and Bow Echoes. Part I. Climatol. Distribution. *Wea. Forecasting* 20, 23–34. <https://doi.org/10.1175/WAF-835.1>.
- Weisman, M.L., 1993. The genesis of severe, long-lived bow echoes. *J. Atmos. Sci.* 50, 645–670. [https://doi.org/10.1175/1520-0469\(1993\)050<0645:TGOSLL>2.0.CO;2](https://doi.org/10.1175/1520-0469(1993)050<0645:TGOSLL>2.0.CO;2).
- Weisman, M.L., Klemp, J., 1982. The dependence of numerically simulated convective storms on vertical wind shear and buoyancy. *Mon. Weather Rev.* 110, 504–520. [https://doi.org/10.1175/1520-0493\(1982\)110<0504:tdonsc>2.0.CO;2](https://doi.org/10.1175/1520-0493(1982)110<0504:tdonsc>2.0.CO;2).
- Weisman, M.L., Trapp, R.J., 2003. Low-level mesovortices within squall lines and bow echoes. Part I: overview and sensitivity to environmental vertical wind shear. *Mon. Weather Rev.* 131, 2779–2803. [https://doi.org/10.1175/1520-0493\(2003\)131<2779:LMWSLA>2.0.CO;2](https://doi.org/10.1175/1520-0493(2003)131<2779:LMWSLA>2.0.CO;2).